Global and Target Analysis of Time-Resolved Fluorescence Spectra of Di-9*H*-fluoren-9-yldimethylsilane: Dynamics and Energetics for Intramolecular Excimer Formation

Bong Hyun Boo* and Dongeun Kang

Department of Chemistry, Chungnam National University, Daejeon 305-764, South Korea

Received: October 15, 2004

Dynamics and energetics for intramolecular excimer formation of a diarylsilane, di-9*H*-fluoren-9-yldimethylsilane (DFYDMS) have been investigated by means of ps time-resolved fluorescence spectroscopy and ab initio calculation. Multiple fluorescence decay curves were globally deconvolved to generate time-resolved fluorescence spectra and decay-associated spectra (DAS), from which species-associated spectra (SAS) were obtained. It is shown in the global analysis that there are at least three excited states: Two states are the locally excited (LE) states ($\lambda_{max} \sim 320$ nm) having lifetimes of 0.70 ± 0.04 and 1.75 ± 0.02 ns, and another is the excimer state ($\lambda_{max} \sim 400$ nm) having a lifetime of 7.34 ± 0.02 ns. The species which decays with 0.70 ns evolves into a species with a red-shifted spectrum, which in turn decays in 7.34 ns. The experimental and ab initio results indicate that the rise time of 0.70 ns corresponds to the conversion of the initial S_1 LE state having a near sandwich geometry to the S_1 excimer state adopting a true sandwich geometry.

I. Introduction

It has been shown that diarylalkanes capable of adopting a face-to-face arrangement of two aromatic rings are ideal systems for which to probe intramolecular excimer formation and excimer-dependent photoprocesses.[1−5] In 1991, we reported intramolecular excimer formation dynamics of bis(9-fluorenyl)-methane (BFM), a good example for the intramolecular excimer formation of diaryl compounds.[1] We have shown that BFM exhibits excimer fluorescence in solution at ambient temperatures. An Arrhenius plot of the temperature-dependent excimer formation rate yielded activation energy of about 15 kJ/mol. It has been proposed that the activation energy is related to the barrier for transforming the initial S_1 geometry to the face-to-face (sandwich-pair) geometry of the intramolecular singlet excimer.[1] This is in accord with the study of an intramolecular excimer formation in jet-cooled 1,3-diphenylpropane (DPP),[2] and that of an intramolecular exciplex formation in 1-(9-anthryl)-3-(4-*N*,*N*-dimethylaniline)propane,[6] which indicate that the energy threshold for such conformational change is about 11 kJ/mol. Quite recently, Lee et al. have reported that resonant two-photon ionization of jet-cooled DPP proceeds very efficiently through the formation and ionization of an intermolecular singlet excimer.[5]

The study of interactions between photoactive moieties could provide valuable information on the medium connecting the moieties. A recent study of intramolecular excimer fluorescence of *cis*-1,4-di(1-pyrenyl)decamethylcyclohexasilane could be a good example to study the effect of the flexibility of the silicon ring on the excimer formation rate and to explore how much the spatial separation and the overlap between the chromophores affect the excimer fluorescence intensity.[7] Formation of face-to-face complex is possible in a cis isomer since conformational change of the cyclohexasilane ring can put both pyrenyl groups into an axial position. In the study, weak excimer intensity and slow excimer formation rates (ca. 0.025 ns^{-1}) were observed, reflecting the large separation (approximately 4.0 Å) and reduced overlap between the chromophores and the presence of the less flexible cyclic silicon ring.

We employed a much simpler medium of dimethylsilylene connecting the photoactive fluorenyl units. In this case, the smaller interchromophore separation of ca. 3.3 Å is achieved as a normal value in adopting the sandwich conformation. Although the presence of the $\sigma-\pi$ mixing could hinder a free rotation along the fl−Si bond (where fl refers to a fluorenyl ring), various conformational changes can be attained.

In this paper, we have explored dynamic and energetic behaviors for intramolecular excimer formation of a diarylsilane molecule, DFYDMS, the molecular model of which is depicted in Figure 1. Here we could elucidate how the presence of the silicon atom and two methyl groups affects the dynamics and energetics of the excimer formation through the fl−Si−fl bond rotation and the stability of possible conformers of T-shape, trans−gauche (tg), and gauche−gauche (gg). Note that the replacement of the dimethylsilylene unit in the BFM molecule could bring about restriction of the fl−Si−fl bond rotation presumably owing to the $p_\pi-d_\pi-p_\pi$ hyperconjugation and to steric hindrance possibly arisen from the presence of the two methyl groups.

The steady-state fluorescence spectrum possesses the normal and excimer fluorescences which are not isolated owing to the comparatively very weak intensity of the excimer fluorescence, and thus we performed global[8−16] and target[9,10,16] analysis of the various traces observed in the range from 310 to 400 nm to simultaneously estimate the individual kinetics and amplitudes, from which time-resolved emission spectra (TRES) and DAS can be obtained.[8−16] The advantage of the approach is to establish relationships between individual decays.

It is found in the theoretical calculation that the gg (sandwich) conformer is found to be a local minimum in our ab initio calculation on the electronically ground state of DFYDMS,

* To whom correspondence should be addressed. E-mail:bhboo@cnu.ac.kr. Fax:82-42-821-8896.

10.1021/jp0406621 CCC: $30.25
Published on Web 04/21/2005

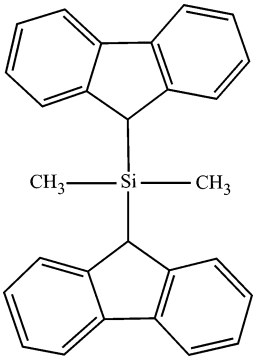

Figure 1. Molecular model of di-9*H*-fluoren-9-yldimethylsilane.

whereas the sandwich conformer of BFM is found to be, however, not a local minimum.[17] Comparison of the computed total energy of the T-shape conformer of DFYDMS with that of the sandwich pair could provide relative number densities of the two states and also predict a lower limit (due to possible presence of the reverse energy barrier) of the activation barrier for the conformation change that takes the initial geometry of the T-shape conformer to the final sandwich geometry in the ground state.

II. Experimental and Theoretical Methodologies

Temporal profiles of the fluorescence decays were measured by using the time-correlated single photon counting (TCSPC) method. The excitation source is a self-mode-locked picosecond Ti:Sapphire laser (Coherent Co.) pumped by a Nd:YVO_4 laser. Laser output has a 3 ps pulse width, and it can span the excitation wavelength in the ranges 235−300 and 350−490 nm by using nonlinear optical crystals. The resultant fwhm is 60 ps. This method allows a time resolution of about 20 ps after deconvolution. The instrumental response function was measured by detecting the scattered laser pulse of ca. 1 ps using a quartz crystal. All the standard electronics for the TCSPC experiment were purchased from the Edinburgh Instruments. The sample DFYDMS with a nominal purity of 97% was purchased from Aldrich Chemical Co. and used without further purification.

The single photon counting data were fitted with a sufficient number of exponential decays and their amplitude,[10,18] which constitute the DAS, as shown in eq 1.[8−16]

$$f(\lambda, t) = \sum_i \mathrm{DAS}(\lambda, k_i)\exp(-k_i, t) = \sum_i f_i(\lambda, t) \qquad (1)$$

where $f(\lambda, t)$ is the deconvolved total fluorescence intensity at wavelength λ at time t after δ-pulse irradiation, and $f_i(\lambda, t)$ is the individual intensity corresponding to "i" species.

If the deconvolved decays at each wavelength were presented as

$$f^{obs}(\lambda, t) = \sum_i n_i(\lambda)\exp(-w_i t) \qquad (2)$$

where $\sum|n_i(\lambda)| = 1$, the DAS was then calibrated using the steady-state fluorescence spectra as

$$\mathrm{DAS}(\lambda, w_i) = n_i(\lambda)F^{ss}(\lambda)/\sum_i \frac{n_i(\lambda)}{w_i} \qquad (3)$$

where $F^{ss}(\lambda)$ is the total steady-state fluorescence intensity.

The ground-state equilibrium geometry of DFYDMS was probed by Kohn−Sham density functional theory (DFT).[19]

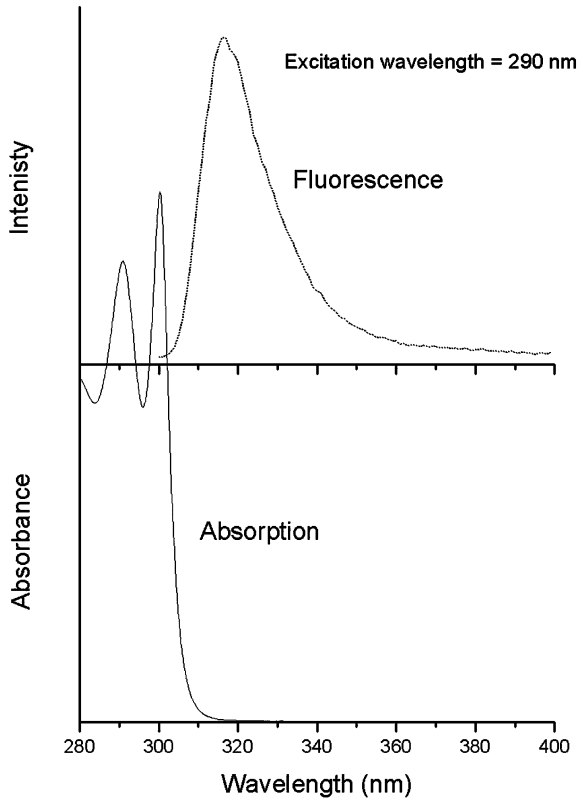

Figure 2. Absorption and fluorescence spectra of di-9*H*-fluoren-9-yldimethylsilane in a 1.0×10^{-4} M solution in cyclohexane.

Becke's three-parameter exchange functional[20,21] and the gradient-corrected Lee−Yang−Parr correlational functional (B3LYP)[22] were used with the 6-31G* basis set. Single point energy calculations at the MP2/6-31G*[23−25] and DFT B3LYP/6-31G* levels of theory were performed on the DFT B3LYP/6-31G*-optimized geometries for computing the relative energies of the various low-energy conformers. The zero-point energy (ZPE) corrections were performed on the electronic energy by using the scale factor of 0.963 used for B3LYP/6-31G*, as described by Rauhut et al.[26] and Boo et al.[27] Also, thermal corrections were performed on the total (electronic and vibrational) energies. All calculations were carried out with the Gaussian 98 suite of program[28] installed at KISTI in Korea.

III. Results and Discussion

A 1.0×10^{-4}M DFYDMS solution in cyclohexane shows two absorptions at 290.8 and 300.2 nm. When the solution was excited at 287 nm, a red-shifted fluorescence of $\lambda_{max} = 317$ nm is observed, having a long tail ranging up to about 400 nm, the broad spectral phenomenon has also been observed in the fluorescence spectrum of BFM.[1] Figure 2 shows the absorption and fluorescence spectra of DFYDMS.

Owing to overlap of the possible spectral regions for the normal and excimer fluorescence, and to relatively weak emission intensity of the 400 nm component, we measured the decay curves at the various wavelengths in the range from 310 to 400 nm. As presented in Figure 3, the 310, 320, and 330 nm traces are commonly observed to decay, having a fluorescence lifetime of 1.75 ns, and the 390 and 400 nm traces are found to rise (rise time = 0.70 ns) after the irradiation pulse and then to decay, having a lifetime of 7.34 ns. We collected fluorescence light for longer time for some weakly fluorescent species such as the 400 nm component and then arbitrarily scaled the spectral intensities for better comparison. When we monitored interme-

TABLE 1: Kinetics and Dynamics of Electronically Excited State (S_1 State) of a Di-9*H*-fluoren-9-yldimethylsilane Solution in Cyclohexane

excited species	monomer state	monomer state	excimer state
lifetime (ns)[a]	0.70(0.04)	1.75(0.02)	7.34(0.02)
structure	near face-to-face	orthogonal and trans−gauche	face-to-face
max of fluorescence wavelength (nm)	∼320	∼320	∼400
state of destination	excimer state	S_0 state having an orthogonal or trans-gauche structure	S_0 having a near face-to-face structure

[a] The values in parentheses are the uncertainties related to the estimation of the kinetic parameters by a global analysis.

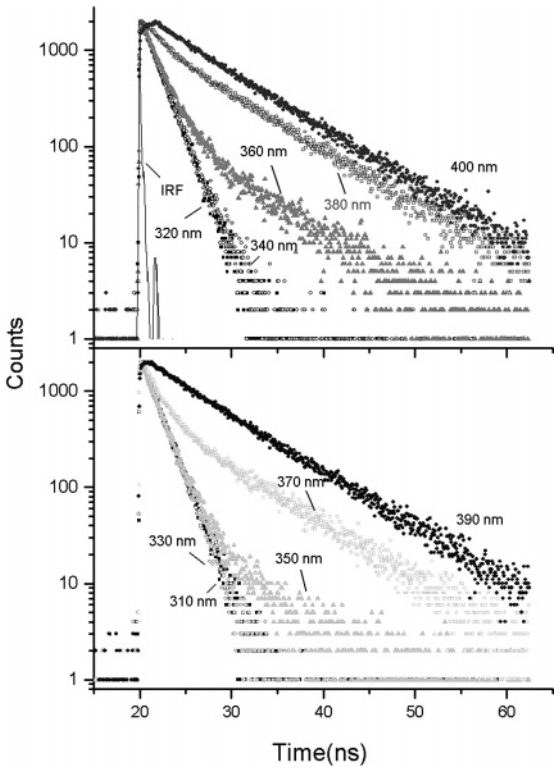

Figure 3. Ten traces of time-resolved fluorescence of a 2.2×10^{-5} M di-9*H*-fluoren-9-yldimethylsilane solution in cyclohexane in the range from 310 to 400 nm. Excitation wavelength = 287 nm, monitoring wavelengths are shown in the respective graphs. Fluorescence intensities are scaled for better comparison.

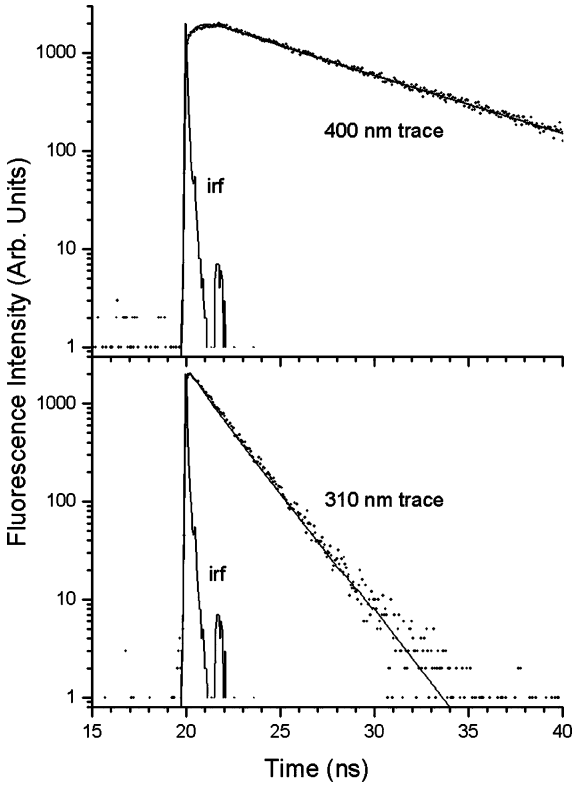

Figure 4. Fits of two traces at critical wavelengths of 310 and 400 nm.

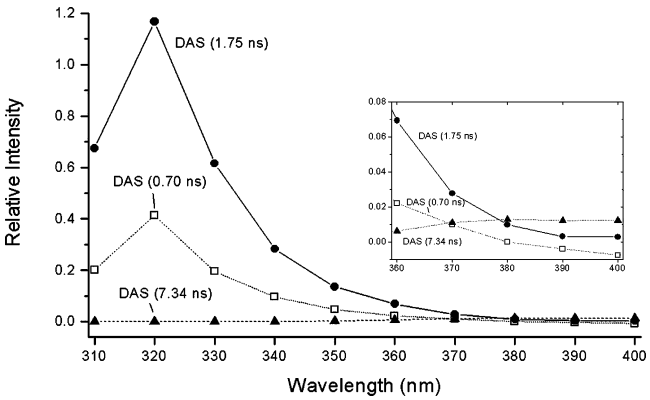

Figure 5. Calculated decay-associated spectra. The inset shows the scale-expanded spectrum.

diate wavelengths in order to check whether the 400 nm trace is really at least one independent excited species or not, and to estimate the fluorescence wavelength ranges covered by the monomer and excimer components, the time-dependent decay function associated with the intermediate 350, 360, and 370 nm traces was found to consist of at least two exponential components. One is the short component having approximately $\tau_F = 1.75$ ns, and the other is the longer component having lifetimes of about 7.34 ns. Therefore, we presume that the nonzero fluorescence intensities observed in the range from about 350 to about 370 nm (Figure 2) arises from the tails of the normal or excimer fluorescence and from the spectral overlap.

To fully extract the reliable kinetic and dynamic information from the complex dynamic system, we carried out global analysis of the 10 traces shown in Figure 3. The model parameters such as rate constants and spectra can be estimated from the data, thereby providing a concise description concerning the complex system dynamics. The global analysis results indicate that the 10 traces (from 310 to 400 nm) shown in Figure 3 can be well described by three lifetimes of 0.70 ± 0.04, 1.75 ± 0.02, and 7.34 ± 0.02 ns. The kinetic parameters with which the excited reactions are undergoing are described together with the corresponding structures in Table 1. Two data fits at the critical wavelengths of 310 and 400 nm are presented in Figure 4. The amplitudes used for the fit were calibrated with the total steady-state fluorescence. The resulting calibrated DAS and SAS are presented in Figures 5 and 6, respectively. The DAS of the 0.70 ns species possesses negative amplitudes at 390 and 400 nm, which is the region where the 7.34 ns possesses maximal amplitudes. This is a strong indication that the species which

TABLE 2: Electronic, Zero-Point, and Relative Energies of nearly Orthogonal, Trans−Gauche, and Gauche−Gauche Forms of Di-9*H*-fluoren-9-yldimethylsilane Calculated with Various Levels of Theory at the Geometries Optimized with the DFT B3LYP/6-31G* Method

conformer	electronic energy (hartree) B3LYP/6-31G(d)	electronic energy (hartree) MP2/6-31G(d)	ZPE[a] (hartree) B3LYP/6-31G(d)	thermal correction to energy at 298 K (kJ/mol)[b] B3LYP/6-31G(d)	relative energy (kJ/mol) at 298 K B3LYP/6-31G(d)	relative energy (kJ/mol) at 298 K MP2/6-31G(d)	entropy (J/(mol·K)) B3LYP/6-31G(d)	thermal correction to Gibbs free energy at 298 K (kJ/mol)[c] B3LYP/6-31G(d)	relative Gibbs free energy (kJ/mol) at 298 K B3LYP/6-31G(d)	relative Gibbs free energy (kJ/mol) at 298 K MP2/6-31G(d)
nearly orthogonal	−1371.003940	−1366. 941971	0.4166391	63.7	0	0	699.8	−142.4	0	0
trans−gauche	−1371.000933	−1366.940366	0.4165851	63.4	7.5	3.8	701.7	−143.3	6.9	3.2
gauche−gauche (sandwich)	−1370.996243	−1366.938487	0.4162490	63.4	18.9	7.8	693.1	−140.8	20.9	9.8

[a] Scaled by 0.963. [b] Contribution from translational, rotational and vibrational energies except the zero-point energy at 298.15. [c] Contribution from internal energy (except the zero-point energy), enthalpy, and Gibbs free energy at 298 K.

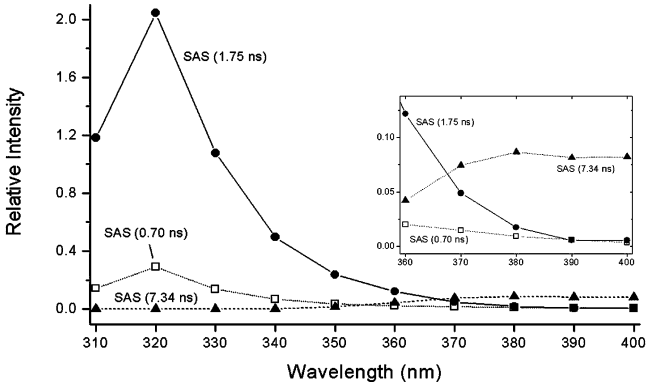

Figure 6. Calculated species-associated spectra. The inset shows the scale-expanded spectrum.

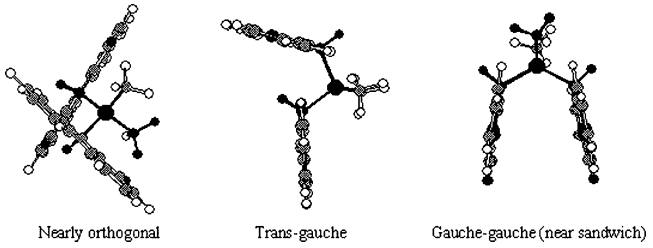

Figure 7. Three possible conformers predicted as stable species in the ground-state DFYDMS by the DFT B3LYP/6-31G* calculations.

decays with 0.70 ns evolves into a species with a red-shifted spectrum, which in turn decays in 7.36 ns.

Similar dynamics has also been reported recently in the *cis*-1,4-di(1-pyrenyl)decamethylcyclohexasilane.[7] The DAS of the state having a 14 ns lifetime is found to be negative in the range 460−540 nm, in which the DAS of the excimer state having 50 ns appears to increase slightly, indicating that the species emitting at long wavelength is formed from the species emitting at short wavlengths with the apparent time constant (i.e., the species which decays with 14 ns evolves into a species), which decays in 50 ns. The conformational change with these time constants describes the intramolecular excimer formation of *cis*-1,4-di(1-pyrenyl)decamethylcyclohexasilane. In the study, Walree et al. suggested that the equilibrium is present between the species emitting at these wavelengths the short and long wavelengths.[7]

On the basis of the observation of the negative amplitudes, we performed a target analysis where the two species of 0.70 and 1.75 ns are excited. It is shown that the shape of the 0.70 ns SAS is equal to the sum of the 0.70 and 7.34 ns DAS. This also indicates that the species with the 0.70 ns lifetime decays and forms the species which diminishes in 7.34 ns.

One can naturally take up questions regarding where the LE state having the near sandwich geometry fluoresces, and if the fluorescence wavelength is close to 317 nm, why not we clearly observe the short decay component of 0.70 ns in the decay curves (Figure 3). This is presumably because the density of the near sandwich conformer is much lower than those of the T-shape and tg conformers, being reflected from the relatively high energy of the gg conformer (vide infra in the theoretical consideration and Table 2).

In BFM, the fluorescence lifetime of the LE state (310 nm) is correlated with the rate constants of $k_r + k_{nr} + k_{ex}$ as given in eq 4, being found to be much longer, with $\tau = 4.6$ ns, than that in DFYDMS.[1]

$$1/\tau_F = k_r + k_{nr} + k_{ex} \quad (4)$$

Here, k_r refers to the radiative decay rate constant, k_{nr} to the nonradiative decay rate constant excluding the intramolecular excimer formation process, and k_{ex} to the excimer formation rate constant. The excimer formation rate constant (k_{ex}) can be calculated to be 1.2×10^8/s from eq 1 and $1/(k_r + k_{nr}) = \sim 10$ ns.[29]

The rise time of the intramolecular excimer of BFM is 4.2 ns, being shorter than $1/k_{ex}$(= 8.3 ns). This indicates that there exists another fast channel for forming intramolecular excimer, which may involve processes converting a near sandwich pair LE state to the excimer state.

In DFYDMS, if we assume that $1/(k_r + k_{nr}) = \sim 10$ ns, we obtain $k_{ex} = 4.7 \times 10^8$/s because $\tau_F = 1.75$ ns. The rise time of the excimer state of DFYDMS is found to be 0.70 ns for the cyclohexane solution, being much shorter than $1/k_{ex}$ (=2.1 ns). Thus, we presume that the rise time of 0.70 ns in the time-dependent fluorescence spectrum of the 400 nm trace corresponds to the conformational change from the near sandwich geometry to the true face-to-face arrangement. The decay time of the intramolecular excimer of BFM (390 nm) is found to be much longer, being $\tau = 29$ ns, than that of DFYDMS. The longer decay time has been suggested as a characteristic feature of the excimer state.[1,30]

At least, three conformers having the nearly orthogonal (T-shape), tg, and gg (near sandwich) geometries were predicted as stable conformers by full optimizations using the DFT B3LYP/6-31G(d) method (Figure 7). Single-point calculations with the MP2/6-31G(d)//DFT B3LYP/6-31G(d) and DFT B3LYP/6-31G(d)//DFT B3LYP/6-31G(d) methods predict that the nearly orthogonal conformer (near T-shape) is most stable (Table 2). A MP2/6-31G(d)//DFT B3LYP/6-31G(d) calculation on BFM also predicts that that the T-shape conformer is most stable (more stable than the tg conformer by 3.8 kJ/mol.[27]) However, the sandwich conformer is not predicted as a local minimum in

the geometry optimization of the electronically ground state of BFM. The total-energy differences of 18.9 (DFT) and 7.8 kJ/mol (MP2) between the T-shape and near sandwich conformers of the electronically ground states of DFYDMS could be a lower limit of the energy barrier for the conversion of the nearly orthogonal geometry to the near-sandwich geometry in the ground state of DFYDMS.

By the aid of this ab initio study, we presume that the rise time of 0.7 ns may correspond to the excimer formation from the near sandwich conformer shown in Figure 7 to a true sandwich conformer in which a face-to-face arrangement of the two aromatic rings is achieved. The finding underscores the important role the excited states of aromatic dimers play (as electron donors) in chemical and biological electron-transfer processes.

IV. Conclusions

Multiple fluorescence decay curves were globally deconvolved to generate time-resolved emission spectra and decay-associated spectra, from which the species-associated spectra were obtained. The global analysis indicates that there are at least three excited states: Two states correspond to the locally excited (LE) states ($\lambda_{max} \sim 320$ nm) having lifetimes of 0.70 ± 0.04 and 1.75 ± 0.02 ns, and another is the excimer state ($\lambda_{max} \sim 400$ nm) having a lifetime of 7.34 ± 0.02 ns. The DAS and SAS results indicate the species which decays with 0.70 ns evolves into a species with a redshifted spectrum, which in turn diminishes in 7.34 ns.

As indicated in the ab initio study, the molecule is presumed to have at least the three minima in the electronically ground states. The LE states may correspond to one of the orthogonal, tg, and near face-to-face geometries, whereas the excimer state may correspond to the face-to-face arrangement. By the aid of the ab initio calculation, we presume that the rise time of about 0.70 ns corresponds to the conversion of the initial S_1 LE state having a near sandwich geometry to the S_1 excimer state adopting a true sandwich geometry.

Acknowledgment. This work was supported by a Korea Research Foundation Grant (KRF-2001-041-D00115), which is greatly acknowledged. Professor van Stokkum helped us in carrying out the global and target analysis of the time-resolved spectra, which is greatly acknowledged. We are very grateful to the KISTI Supercomputer Center in South Korea for a generous grant of the computation time.

References and Notes

(1) Chung, Y. B.; Jang, D.-J.; Kim, D.; Lee, M.; Kim, H. S.; Boo, B. H. *Chem. Phys. Lett.* **1991**, *176*, 453.

(2) Chakraborty, T.; Lim, E. C. *J. Phys. Chem.* **1995**, *99*, 17505.

(3) Cid-Aguero, P.; Liu, H.; Lim, E. C. *Chem. Phys. Lett.* **1997**, *280*, 489.

(4) East, A. L. L.; Cid Aguero, P.; Liu, H.; Judge, R. H.; Lim, E. C. *J. Phys. Chem. A* **2000**, *104*, 1456.

(5) Lee, J. K.; Judge, R. H.; Boo, B. H.; Lim. E. C. *J. Chem. Phys.* **2002**, *116*, 8809.

(6) Syage, J. A.; Felker, P. M.; Zewail, A. H. *J. Chem. Phys.* **1984**, *81*, 2233.

(7) van Walree, C. A.; Kaats-Richters, V. E. M.; Jenneskens, L. W.; Williams, R. M.; van Stokkum, I. H. M. *Chem. Phys. Lett.* **2002**, *355*, 65.

(8) Knutson, J. R.; Walbridge, D. G.; Brand, L. *Biochemistry* **1982**, *21*, 4671.

(9) Löfroth, J.-E. *J. Phys. Chem.* **1986**, *90*, 1160.

(10) van Stokkum, I. H. M.; Larsen, D. S.; van Grondelle, R. *Biochim. Biophys. Acta* **2004**, *1657*, 82.

(11) van Stokkum, I. H. M.; Scherer, T.; Brouwer, A. M.; Verhoeven, J. W. *J. Phys. Chem.* **1994**, *98*, 852.

(12) Knutson, J. R.; Beechem, J. M.; Brand, L. *Chem. Phys. Lett.* **1983**, *102*, 501.

(13) Beechem, J. M.; Ameloot, M.; Brand, L. *Anal. Instrum.* **1985**, *14*, 379.

(14) Beechem, J. M.; Ameloot, M.; Brand, L. *Chem. Phys. Lett.* **1985**, *120*, 466.

(15) Beechem, J. M. *Chem. Phys. Lipids* **1989**, *50*, 237.

(16) van Stokkum, I. H. M.; Beekman, L. M. P.; Jones, M. R.; van Brederode, M. E.; van Grondelle, R. *Biochemistry* **1997**, *36*, 11360.

(17) Boo, B. H. Unpublished work.

(18) Knorr, F. J.; Harris, J. M. *Anal. Chem.* **1981**, *53*, 272.

(19) Kohn, W.; Sham, L. J. *Phys. Rev. A* **1965**, *140*, 1133.

(20) Becke, A. D. *Phys. Rev. A* **1998**, *38*, 3098.

(21) Becke, A. D. *J. Chem. Phys.* **1993**, *98*, 5648.

(22) Lee, C.; Yang, W.; Parr, R. G. *Phys. Rev. B* **1988**, *37*, 785.

(23) Head-Gordon, M.; Pople, J. A.; Frisch, M. J. *Chem. Phys. Lett.* **1988**, *153*, 503.

(24) Frisch, M. J.; Head-Gordon, M.; Pople, J. A. *Chem. Phys. Lett.* **1990**, *166*, 275.

(25) Frisch, M. J.; Head-Gordon, M.; Pople, J. A. *Chem. Phys. Lett.* **1990**, *166*, 281.

(26) Rauhut, G.; Pulay, P. *J. Phys. Chem.* **1995**, *99*, 3093.

(27) Boo, B. H.; Park, J.; Yeo, H. G.; Lee, S. Y.; Park, C. J.; Kim, J. H. *J. Phys. Chem. A* **1998**, *102*, 1139.

(28) Frisch, M. J.; Trucks, G. W.; Schlegel, H. B.; Scuseria, G. E.; Robb, M. A.; Cheeseman, J. R.; Zakrzewski, V. G.; Montgomery, J. A., Jr.; Stratmann, R. E.; Burant, J. C.; Dapprich, S.; Millam, J. M.; Daniels, A. D.; Kudin, K. N.; Strain, M. C.; Farkas, O.; Tomasi, J.; Barone, V.; Cossi, M.; Cammi, R.; Mennucci, B.; Pomelli, C.; Adamo, C.; Clifford, S.; Ochterski, J.; Petersson, G. A.; Ayala, P. Y.; Cui, Q.; Morokuma, K.; Malick, D. K.; Rabuck, A. D.; Raghavachari, K.; Foresman, J. B.; Cioslowski, J.; Ortiz, J. V.; Baboul, A. G.; Stefanov, B. B.; Liu, G.; Liashenko, A.; Piskorz, P.; Komaromi, I.; Gomperts, R.; Martin, R. L.; Fox, D. J.; Keith, T.; Al-Laham, M. A.; Peng, C. Y.; Nanayakkara, A.; Challacombe, M.; Gill, P. M. W.; Johnson, B.; Chen, W.; Wong, M. W.; Andres, J. L.; Gonzalez, C.; Head-Gordon, M.; Replogle, E. S.; Pople, J. A. *Gaussian 98*, Revision A.7. Gaussian, Inc: Pittsburgh, PA, 1998.

(29) Lee, M.; Hochstrasser, R. M. *Chem. Phys. Lett.* **1988**, *153*, 1.

(30) Saigusa, H.; Lim, E. C. *Acc. Chem. Res.* **1996**, *29*, 171.